

The Life Cycle and Fitness of Gregarine (Apicomplexa) Parasites

David Logan* & John Janovy, Jr.
Department of Mathematics & School of Biological Sciences
University of Nebraska Lincoln

February 9, 2011

Abstract

Theoretical demographic models with an accompanying experimental program provide an important framework to study the life history of organisms. In this paper we seek to understand the fitness characteristics of gregarine parasites and how they are shaped by their own life cycle stages inside and outside an insect host. The population model is a continuous time dynamics for the parasite stages, and we examine stability and bifurcation of its equilibria for different production rates. Analysis leads to a key fitness parameter whose value determines the existence of a coexistent state. The model shows good cause for the establishment and long time permanence of this common parasite. The model is parameterized by extensive data gathered at Cedar Point Biological Station in western Nebraska, and numerical calculations based on those parameters illustrate the dynamics.

Keywords: Parasites (*Apicomplexa*), population dynamics, fitness.

1 Introduction

Parasitism is perhaps the most common way of life on Earth because every species of plant and animal that has been studied seriously has been shown to be parasitized by at least one, and often several, non-related species of protists, fungi, plants, or animals (Roberts and Janovy, 2009). Host-parasite systems are enormously varied with respect to modes of transmission, physiological relationships between the species, and infection sites, and many are of serious economic importance. Thus it is not surprising that both experimental and theoretical research on host-parasite interactions is extensive.

*Communicating author: Department of Mathematics, University of Nebraska Lincoln, Lincoln, NE 68588-0130.

In this paper we focus on macroparasites and their insect hosts. In contrast to microparasites like viruses and bacteria, macroparasites have longer generations times, are larger, have at least one life cycle stage outside the host, and do not multiply in the infective stage within the host. Good examples of macroparasites include helminths such as tapeworms and arthropods such as fleas and ticks. Typically, macroparasite infections are aggregated, with most individual parasites occurring in a relative few host individuals and a large number of hosts being either lightly- or non-infected. Consequently, macroparasite populations often are described by negative binomial distributions in which variance-to-mean ratios are large, and quantitative models most often focus on parasite infrapopulations (number of parasites per host = $0-\infty$) instead of prevalence (fraction of hosts infected) (Nodvedt et al., 2002; Pal and Lewis, 2004).

Host-parasite interactions in aquatic environments have not been modeled to the same extent as terrestrial ones of economic importance, but within the past few decades, with growing importance of aquaculture, efforts to control disease vectors, and impact of climate change, there has been increasing interest in such systems (Milner & Patton, 1999; Marcogliese, 2001; Esteva et al., 2006; Fenton et al., 2006; Revie et al., 2007). Parasites vary considerably in their dependence upon aquatic environments, ranging, for example, from trematodes that generally require molluscs as first intermediate hosts and live for a short time outside their hosts, to malarial parasites transmitted by vectors with aquatic life cycle stages. Aside from their economic importance, therefore, aquatic hosts offer many opportunities to explore avenues for, and constraints on, evolutionary change (Bolek & Janovy, 2007; 2007a). And among the most common and diverse of host-parasite systems in aquatic environments are ones involving invertebrates and the so-called "gregarines" (Levine, 1988; Clopton, 2000).

Gregarine parasites (phylum Apicomplexa; class Conoidasida; order Eugregarinorida) are large, single-celled, eukaryotes that are transmitted by oocysts ingested by a host. All invertebrate phyla have been reported as hosts for gregarines, but they are most numerous in arthropods and annelids. Beetles alone (order Coleoptera) are infected with one to two species of gregarine per host species, leading to a reasonable estimate of approximately 500,000 gregarine species in coleopterans. Damselflies and dragonflies (order Odonata; "odonates") also have a rich gregarine fauna, with several species often occurring in single host species in a single collection site (Clopton et al., 1993; Percival et al., 1995). Differences in larval and adult odonate habitats, prey species, behaviors (including sex-specific mating behaviors), and potential for geographic distribution, as well as differences in parasite species' structure and development, all provide rich opportunities for using these insects as model systems for studying macroparasite population dynamics, especially in an evolutionary context.

A typical gregarine life cycle is direct, with numerous developmental stages both inside and outside the hosts (**Fig. 1**). Hosts ingest oocysts, containing infective sporozoites, which attach to or penetrate hosts' intestinal epithelium cells. Subsequent growth stages known as trophozoites eventually detach from

the epithelium and form associations with parasite cells of different mating types, thus becoming gamonts, which undergo syzygy and secrete a gametocyst. The latter are usually shed into the environment where gamonts undergo schizogony, forming gametes, which unite, forming zygotes. These zygotes then secrete an oocyst wall and go through zygotic meiosis to form haploid infective sporozoites, which are then released from the gametocyst by a variety of mechanisms known collectively as dehiscence. A gametocyst may produce several thousand oocysts, each containing eight sporozoites.

This paper concerns our efforts to establish insect-gregarine systems as models for host-parasite interaction dynamics, and especially to inspire comparative work leading to evolutionary hypotheses. Our immediate goal is to formulate a continuous-time, mathematical model (differential equations) of this process under some simplifying assumptions. Our aim is to understand factors affecting parasite fitness in nature, with special focus on the interplay among basic parameters of reproduction rates, infection rates, mortality, and host populations. One key assumption is that the host population is constant. This assumption is not an uncommon one in infectious disease models (Anderson & May, 1978; Dobson 1989; Anderson & May, 1991; Dobson & Hilton, 1992; Mangel, 2006). We also assume that damselflies are not affected by gregarines, a position consistent both with the idea that well-adapted parasites are relatively harmless to their hosts (Nowak, 2006), and with studies that demonstrate little if any negative impact on insect hosts by Eugregarinorida (see Klingenberg et al., 1997; Hecker et al., 2002; Canales-Lazcano et al., 2005; Rodriguez and Omoto, 2007).

We track two parasite stages, the free-living infectious stage (oocysts), and trophonts living in the definitive host (*Ischnura verticalis*, Odonata, Coenagrionidae). Our model represents a simplification of many classical models such as those presented or reviewed by Anderson and May (1978; 1991), Dobson (1989), Dobson and Hilton (1992), Mangel (2006), and many others.

To paraphrase Maynard-Smith (1974, p. 35), the value of a theoretical population model is not in a precise description of the biological situation or in its ability, or inability, to predict population abundances exactly. What we do ask, in fact, is what kind of change in the behavior of our model is made by a particular change in parameters; the assumption is that a comparable change will occur in the behavior of a real biological system. This brings up the issue of structural stability of the model with respect to changes in parameters. We want to know which parameters are critical and which are not. A common approach is to select a fixed set of baseline parameters and perform a baseline simulation of the dynamics; the magnitude of the change is measured from the baseline.

Specifically we want to understand the fitness characteristics and longevity of gregarine parasites and how they are shaped by their own life stages inside and outside a definitive insect host. The population model is a system of differential equations for the parasite stages (the trophonts in the definitive host and the free-living infectious oocysts), and we examine its possible equilibria under change of key life history parameters. A stability analysis leads to values that characterize population fitness and give good cause for the establishment

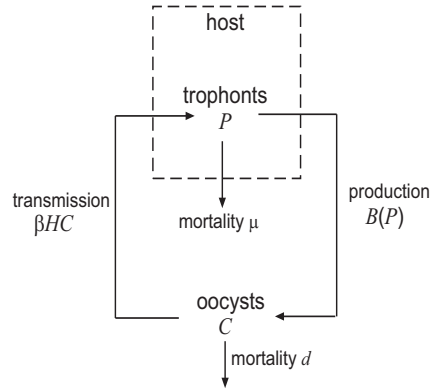


Figure 1: Simplified continuous life-cycle of the typical gregarine parasite showing the rates between the trophont and oocyst stages.

Table 1: Definitions of Quantities

Quantity	Description and Units
$P(t)$	parasite load (per host)
$C(t)$	oocysts (per host)
H	host population (constant)
β	infection/ingestion rate (per host, per day)
μ	trophont mortality rate (per day)
d	oocyst mortality rate (per day)
b	saturating production rate (per day, per host)
γ	half-saturation (per host)

and long time permanence of these common parasites. The model is parameterized by extensive data gathered at Cedar Point Biological Station in western Nebraska, and numerical calculations and bifurcation analysis based on those parameters illustrate the dynamics.

2 Model Formulation

The simplified gregarine life cycle is shown in fig. 1. It tracks the trophonts and oocysts, $P(t)$ and $C(t)$, respectively, where t is time given in days. Both P and C are measured in units of ‘per host’. Therefore, we think of $P(t)$ as the parasite load. We let H denote the constant number of hosts. Referring to the life cycle diagram in fig. 1, we make the following assumptions. For reference, we can refer to Table 1 for the meaning of the quantities introduced.

The rate of change of the parasite load is due to ingestion of oocysts and their natural mortality in the gut lumen. In symbols,

$$\frac{dP}{dt} = \beta HC - \mu P, \quad (1)$$

where μ is the natural mortality of trophonts and β is the ingestion rate of infective oocysts. Thus, $1/\mu$ is the average lifespan of a trophont.

The oocysts, per host, are increased by the production of oocysts through the gametogenesis process, and they are decreased by natural mortality in the environment and consumption by the hosts. Therefore,

$$\frac{dC}{dt} = B(P) - dC - \beta HC, \quad (2)$$

where d is the natural mortality of trophonts and $B(P)$ is the production rate (per time per host) of infective oocysts. Thus, $1/d$ is the average lifespan of a oocyst.

Momentarily we discuss the form of the production rate. First, however, we note that the mortality rates may include other losses, for example, from predation or removal from the system. The ingestion rate, βHC , is a type 1, or mass-action response. The product HC is the number of possible encounters between hosts and oocysts; the constant β represents the product of the fraction of encounters that actually occur and the fraction of effective encounters that lead to ingestion of the infective stage.

The model (1)–(2) can be analyzed using many forms for the constitutive assumption for the production rate. Generally, all that is required analytically is that $B(P)$ be a nonnegative smooth function for $P \geq 0$ with the properties

$$B(0) = 0, \quad B'(0) = 0, \quad B'(P) > 0 \text{ for } P > 0,$$

and

$$\lim_{P \rightarrow \infty} B(P) = b > 0.$$

Thus, we require that $B(P)$ be an increasing, saturating function. For our specific analysis, we choose a type 3 functional response,

$$B(P) = \frac{bP^2}{\gamma^2 + P^2}, \quad (3)$$

where $b > 0$ is the saturating value and γ is the half-saturation, or $B(\gamma) = \frac{1}{2}b$. Such a functional response implies a small rate of production when the trophont population is small (difficulty in finding mates), and a saturated rate when the population is large (crowdedness in the small insect gut).

Now we present a brief argument why we take this form for the production rate. First, from a quantitative modeling viewpoint, we observe that general higher-order functional responses, e.g.,

$$B(P) = \frac{bP^m}{\gamma^m + P^m}, \quad m > 2, \quad (4)$$

satisfy the same requirements listed above and lead to a similar analysis and to qualitatively the same results that we find in the next section. The difference is that for larger values of the exponent m , compared to $m = 2$, the curve has a quicker, faster rise to the saturation value; this rise occurs near the half-saturation density, and so high values of m lead to a more well defined threshold. A type 2 Holling functional response, when $m = 1$, has a positive slope and a different type of bifurcation and stability properties. If the birth rate is $B(P)$ is proportional to P , then there are no steady-states to the system; the parasite population grows exponentially or becomes extinct. Another possibility is to base the production rate on the dynamics of mating among + and - mating types of trophonts into paired gamonts. If the number of + types and - types in a host each have a Poisson distribution with parameter $P/2$, then the joint distribution of the number of + and - types is

$$\Pr(\text{plus types} = k \text{ and minus types} = l) = e^{-P/2} \frac{(P/2)^{k+l}}{k!l!}.$$

If the number of pairs form by k plus types and l minus types is $\min(k, l)$, the number of pairs is $2 \min(k, l)$; thus, the mean number of paired trophonts in a host is

$$\text{Pairs} = \sum_{k=0}^{\infty} \sum_{l=0}^{\infty} \min(k, l) e^{-P/2} \frac{(P/2)^{k+l}}{k!l!}.$$

For example, see May (1977) or Hoppensteadt (1976). Figure 2 plots this average number, and the plot shows a concave up curve with a near zero slope at the origin. This slope is characteristic of a type 3 response for small parasite populations. Because the plot becomes linearly increasing, a different model would have to be used to predict the saturation in (3) caused by crowdedness.

Therefore, our assumption of a type 3 response (3) leads to several favorable qualitative results. The model is structurally stable, meaning that it holds for a wide variety of parameter values. Therefore, complete accuracy of the parameters is not required; the qualitative predictions are the same. This property is essential in a theoretical, mathematical model where the goal is accurate qualitative results rather than exact numerical predictions (e.g., Maynard-Smith, 1974). Next, the system has interesting bifurcation qualities where a saddle-stable node bifurcates from the extinct state. When the bifurcation occurs, the system migrates quickly to a nonzero stable equilibrium for a large range of parameter values, implying permanence of the gregarine population.

Assumptions. A posteriori, we now summarize the specific assumptions made in the model.

1. The general focus is on parasite fitness, so we have ignored the effects of parasites on their hosts and any possible resulting host immune response. The host population is constant.
2. Pair formation in trophont mating is by chance contact, as are other processes in the formation of oocysts. The model does not express the details of mating.

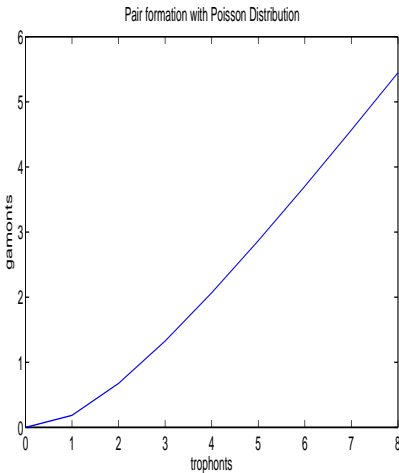


Figure 2: The number of pairs (gamonts) formed from P trophonts. Both plus and minus types of trophonts are assumed to be Poisson distributed.

3. Predation is not directly included. Indirectly, it is incorporated into the natural mortalities. Predation by fish, birds, other predator insects (e.g., dragonfly larva), and other aquatic organisms is a major fact of life for parasites. Further, “wash-out” of parasites in the host gut from fecal elimination is not included directly.
4. Abiotic effects are not considered. These include, for example, temperature, pond inflow and outflow, photoperiod, and environmental gradients.
5. The fact that the parasite load has a negative binomial distribution does not affect our model because we are assuming no mortality of the host (see, e.g., the fundamental models in Anderson & May, 1991).

3 Stability and Bifurcation

In a demographic model it is important to determine the equilibria and their stability properties. We perform the standard stability analysis in a PC phase plane (e.g., see Logan & Wolesensky, 2009). The equilibria are determined by finding the set of values P and C where, simultaneously, $P' = 0$ and $C' = 0$ in (1)–(2). Each of these sets of curves, $P' = 0$ and $C' = 0$, are the isoclines that separate the regions where the trophont population is increasing and decreasing, and the regions where the oocyst population is increasing and decreasing, respectively. In each case (1)–(2) we solve for C to obtain the isoclines

$$C = \frac{\mu}{\beta H} P \quad (P \text{ isocline})$$

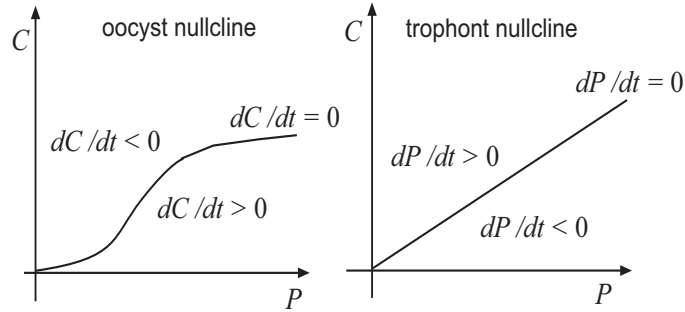


Figure 3: Left: the linear isocline $P' = 0$; right: the isocline $C' = 0$, given by a type 3 functional response (3). The increasing and decreasing nature of the populations P and C are indicated by the sign of the derivatives.

and

$$C = \frac{b}{d + \beta H} \frac{P^2}{\gamma^2 + P^2} \quad (C \text{ isocline})$$

The isoclines are shown and labeled in fig. 3 along with the specific regions where the populations increase or decrease. The equilibria are therefore points in the PC plane where the isoclines intersect. Clearly they can intersect in one point (only the origin, representing extinction), two points (the origin and the point of tangency of the curves), or three points (the origin and two positive values), depending on the slope of the isocline $P' = 0$ and the shape of the isocline $C' = 0$.

Clearly, $P = C = 0$ (the origin, representing extinction) is an equilibrium. Setting the last two equations equal, canceling a factor of P (representing the zero equilibrium), gives a quadratic equation for remaining equilibria, namely,

$$P^2 - \frac{b\beta H}{\mu(d + \beta H)} P + \gamma^2 = 0.$$

The roots are

$$P_{\pm} = P_c \pm \sqrt{P_c^2 - \gamma^2},$$

where

$$P_c = \frac{b}{2\mu} \frac{\beta H}{d + \beta H}.$$

Consistent with the plots, there can be no real roots, one double root, or two real distinct positive roots. The double root P_c , where tangency occurs, is a critical parasite load and occurs when $P_c = \gamma$. When $P_c < \gamma$ there are no nonzero equilibria, and when $P_c > \gamma$ there are two positive equilibria, one less than P_c and one greater than P_c . The three cases are shown in three phase plane diagrams (fig. 4). The direction of the trajectories are indicated by the

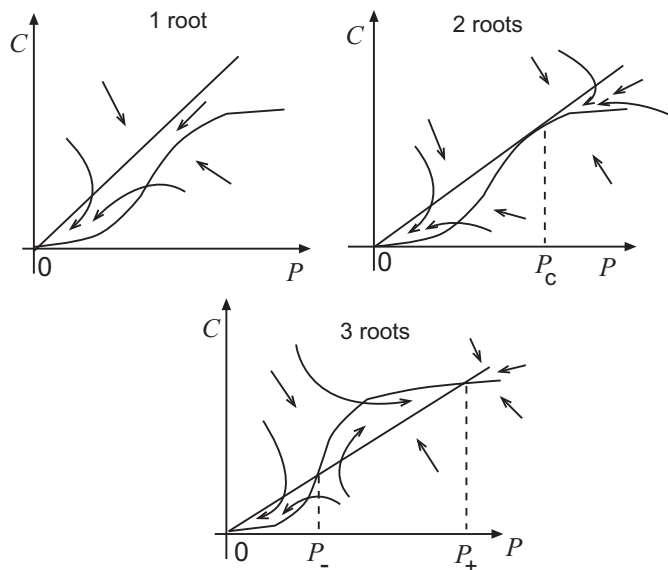


Figure 4: Top left: $P_c < \gamma$. Top right: $P_c = \gamma$. Lower: $P_c > \gamma$. Note that $R = P_c/\gamma$ (see (5)), so these plots may be tagged as $R < 1$, $R = 1$, and $R > 1$.

direction arrows which show where P and C are increasing or decreasing. The isoclines intersect at equilibria.

We can observe geometrically from the trajectories that $P = 0$ is always a stable equilibrium (a node) in all cases, the critical equilibrium P_c is unstable, occurring when $R = P_c/\gamma = 1$, P_- is an unstable equilibrium (a saddle), and P_+ is a stable equilibrium (a node) when $R > 1$. [These facts may be proved by examining the linearization, or Jacobian matrix, of the system near the equilibria.] In Sec. 5 we illustrate the behavior of the model using simulations and the experimental data.

4 Qualitative Results

It is informative to analyze the bifurcation properties, or changes in stability of equilibria caused by changes in a parameter, of (1)–(3) in terms of the parameter R :

$$R = \frac{P_c}{\gamma} = \frac{b}{2\gamma} \frac{1}{\mu} \frac{\beta H}{d + \beta H}, \quad (5)$$

This dimensionless parameter R can be regarded as *fitness*, akin to a basic reproduction number. The three factors making up R are: the average rate $b/2\gamma$ that oocysts are produced by trophonts, the average lifetime $1/\mu$ of trophonts, the transmission rate βH , and the average life time of oocysts plus the average

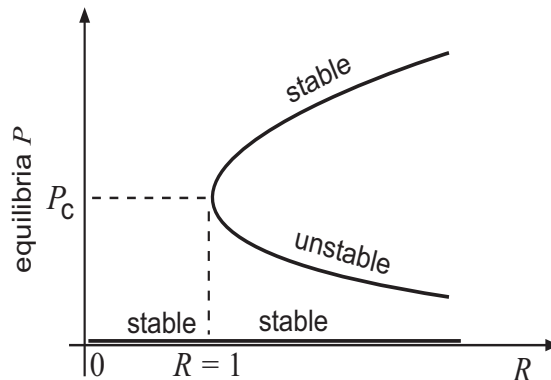


Figure 5: Bifurcation diagram. As the fitness R increases from small values there is a bifurcation at $R = 1$ from the stable, extinct state $P = 0$ to a positive stable node P_+ for $R > 1$. The lower portion of equilibrium curve P_- is unstable.

time to be ingested, $d + \beta H$. We can further write R in terms of two other dimensionless parameters that will show the trade-offs for fitness. Let

$$\theta = \frac{\beta H}{d} \quad (6)$$

and

$$\alpha = \frac{b}{\gamma \mu}. \quad (7)$$

Here, θ is the ratio the transmission rate and the mortality rate of oocysts (properties of the free-living infectious stage) and α is the ratio of the production rate and the trophont mortality rate (properties of the host-residing stage). First, regarding the fitness R as a bifurcation parameter, we can plot the equilibria as functions of R and observe how the equilibria change as the fitness R changes, as described in figure 5.

In terms of the dimensionless parameters θ and α defined in (6)–(7), the *fitness boundary* $R = 1$ is given by

$$\alpha = 2 \left(1 + \frac{1}{\theta} \right), \quad (8)$$

and it is plotted in fig. 6.

An important qualitative result can be deduced in the case $R > 1$ from the phase plane shown in figure 7. There are large regions in PC space where the populations are coexistent and permanent, falling to extinction only at certain threshold values of the parameters. Collectively, figs. 7 and 6 collectively show the structural stability of the model and the well-adaptedness of the parasite population. Beyond a certain threshold value of R there is a global steady state, or limiting population, that is approached regardless of the initial conditions.

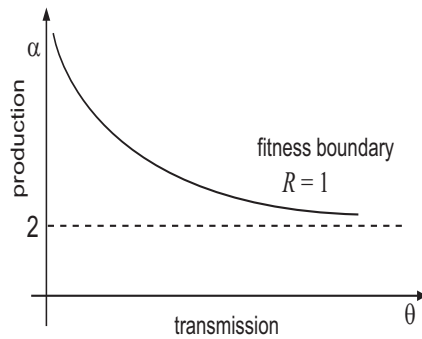


Figure 6: Plot in the $\theta\alpha$ parameter space of the fitness boundary $R = 1$, which is the curve (8) and the region $\alpha > \theta$ of growth and approach to a steady-state equilibrium.

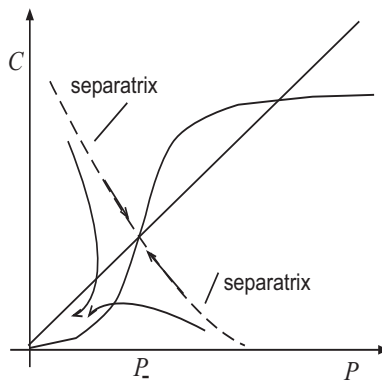


Figure 7: In the case $R > 1$, initial conditions in the region in the first quadrant to the left of the stable manifolds (separatrices) always leads to extinction. Initial conditions to the right of the separatrices lead to permanence, or coexistence. Note that as parameters in the problem change, the values of R change.

We conclude there is a built in mechanism, or trade-off to prevent population explosion of the gregarine parasite.

Dimensionless Formulation. As an interesting aside, the fitness R reveals itself in a natural and unique way if we reformulate the problem in dimensionless form. Taking τ , p , and c as dimensionless variables (time, trophont load, oocysts) defined by

$$t = \mu^{-1}\tau, \quad P = \gamma p, \quad C = \frac{\gamma\mu}{\beta H}c,$$

the model (1)–(3) reduces to

$$\frac{dp}{d\tau} = c - p, \quad \frac{dc}{d\tau} = K \left(\frac{2Rp^2}{1+p^2} - c \right); \quad K \equiv \frac{d + \beta H}{\mu}.$$

The analysis follows easily as before. The equilibria are

$$p = R \pm \sqrt{R^2 - 1},$$

coinciding with our earlier result. As before, there is a positive stable equilibrium when $R > 1$.

As a second note, we comment more carefully on the results when the production rate $B(P)$ is a Holling type 2 response,

$$B(P) = \frac{bP}{\gamma + P}.$$

In this case, using the same dimensionless quantities as above, the model (1)–(2) reduces to

$$\frac{dp}{d\tau} = c - p, \quad \frac{dc}{d\tau} = K \left(R_2 \frac{p}{1+p} - c \right),$$

where K is defined above and the fitness is $R_2 = R/2$, one-half the value of the previous case. Now, the equilibria are $p = 0$ and $p = R_2 - 1$. The latter only exist when $R_2 > 1$, and it is asymptotically stable. It is not difficult to show that extinction is a stable state only when $R_2 < 1$, so there is a change in stability of the extinction state when $R_2 = 1$. A bifurcation diagram summarizes the results and is shown in fig. 8. Again, we obtain a favorable model in that for $R_2 > 1$ there is a positive globally stable coexistent state. Again, our preference in a type 3 response is that the mating model shows positive concavity in that case.

5 Simulations

The experimental efforts and results that form the basis of this study have been documented in detail by Bunker et al., (2011). Briefly, the research was carried out during the summer of 2010. An extensive data set was collected in five

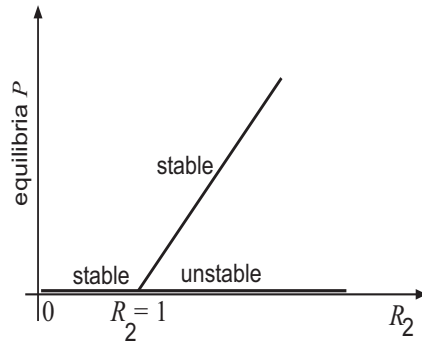


Figure 8: Bifurcation diagram is the case $B(P)$ is a Holling type 2 response. As R_2 increases from a small value there is a bifurcation at $R_2 = 1$ where the extinction state becomes unstable and a new, positive, stable equilibrium appears.

different ponds located just outside Ogallala near Lake McConaughy in Keith County, Nebraska. These particular collection sites were chosen because of their close proximity to Cedar Point Biological Station, and the abundant source of *Ishnura verticalis* larva, teneral, and adults, and a rich population of gregarines infecting these hosts. A series of nine collections were taken from each location, each of which involved collecting a minimum of 50 *Ishnura verticalis* larvae and as many as 53 teneral and 34 adults. Collected specimens were transported to the lab for dissection and measurements and sex determination. Each damselfly was then identified according to Westfall & May (1996). Next each was placed underneath a dissecting microscope and the abdomen of each damselfly was extracted. After removal the gut was removed it was teased apart and placed under the light microscope in order to examine it for the presence of gregarines. If gregarines were seen they were counted and recorded onto a video tape to be identified by species and measured later. Parasites were identified according to the structural criteria defined by Richardson & Janovy (1990), Clopton et al. (1993), and Percival et al. (1995).

The key results of the data collection were:

1. No correlation was found between host size and parasite load. Because host age is directly proportional to body length, this indicates that susceptibility is constant throughout the host's lifetime.
2. The fact that different gregarine species dominate in each of the host stages suggests that parasites are not passed directly, at least in large numbers, during metamorphosis in which a larva are transformed into adults.
3. Gregarine counts in the various stages of the damselflies show a negative binomial distribution in the parasite load. The mean was in the range of

Table 2: Baseline Parameters

Quantity	Baseline value
H	10,000 hosts
β	0.00004 per day, per host
μ	0.8 per day
d	0.4 per day
b	13 per day, per host
γ	3 per host

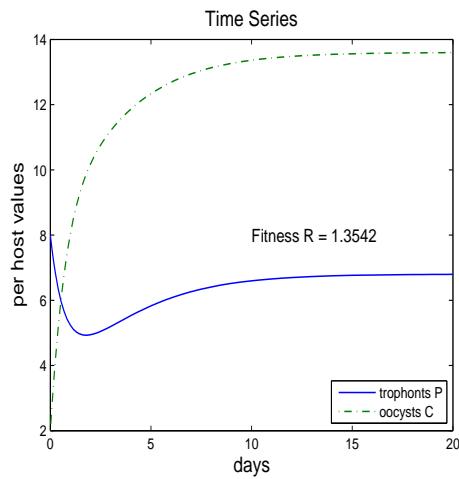


Figure 9: Time series plots $P = P(t)$ of trophonts and $C = C(t)$ of oocysts, showing the approach to steady-state.

5-6 trophonts per host, and the prevalence was found to be near 70% in all collections.

Confronting a model with experimental data is never an easy task. We consider a baseline set of parameters within the scope of our data, which are given in the following table.

The simulations are shown in fig. 9 and 10.

Acknowledgements. This research was funded by a joint grant to the Department of Mathematics and to the School of Biological Sciences at the University

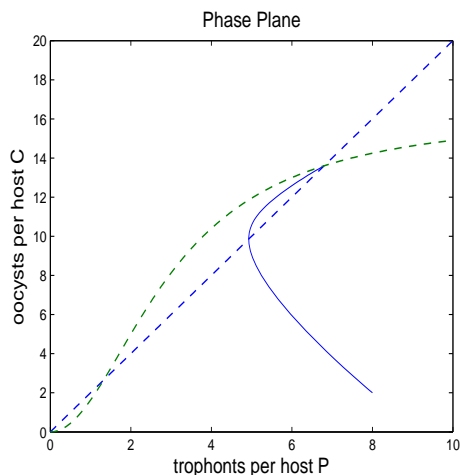


Figure 10: Phase plane plot of the trajectory $(P(t), C(t))$ (solid) approaching the steady state. The isoclines are dashed.

of Nebraska from the National Science Foundation under the BMM (Biological and Mathematical Modeling) program. We are grateful to the grant's faculty administrators, Professors Glenn Ledder (mathematics) and Chad Brassil (biology), for making our RUTE (Research for Undergraduates in Theoretical Ecology) project on parasitology run so smoothly and efficiently.

Participants. Undergraduate RUTE scholars Austin Barnes, Brittany Bunker, Ayla Duba, Matthew Shuman, and Elizabeth Tracey carried out the extensive experimental work at Cedar Point Biological Station.

References

1. Anderson, R. M. & R. M. May. 1978. *Infectious Diseases of Humans*, Oxford University Press, Oxford UK.
2. Bolek, M. G. & J. Janovy, Jr. 2007. Small frogs get their worms first: the role of non-odonate arthropods in the recruitment of *Haematoloechus coloradensis* and *Haematoloechus complexus* in newly metamorphosed northern leopard frogs, *Rana pipiens*, and Woodhouse's toads, *Bufo woodhousii*. *Journal of Parasitology*, 93, 300-312.
3. Bolek, M. G. & J. Janovy, Jr. 2007a. Evolutionary avenues for, and constraints on, the transmission of frog lung flukes (*Haematoloechus* spp.) in dragonfly second intermediate hosts. *Journal of Parasitology*, 93, 593-607.
4. Bunker, B. et al, 2011. In preparation.

5. Canales-Lazcano, J., J. Contreras-Garduno, & A. Cordoba-Aguilar. 2005. Fitness-related attributes and gregarine burden in a non-territorial damselfly *Enallagma praevarumhagen* (Zygoptera: Coenagrionidae). *Odonatologica* 34, 123–130.
6. Clopton, R. E., T. J. Percival & J. Janovy, Jr. 1993. *Nubenocephalus nebraskensis* n. gen., n. sp. (Apicomplexa: Actinocephalidae) from adults of *Argia bipunctulata* (Odonata: Zygoptera). *Journal of Parasitology*, 79, 533-537.
7. Clopton, R. E. 2000. Order Eugregarinorida. In: *An illustrated guide to the protozoa*, 2nd Ed., J. J. Lee, G. F. Leedale, and P. Bradbury (Eds.) p. 205-288.
8. Diekmann, D. & J. A. P. Heesterbeek, 2000. *Mathematical Epidemiology of Infectious Diseases*, John Wiley & Sons, Ltd. Chichester, UK.
9. Dobson, A. P. 1989. The population biology of Parasitic helminths in animal populations, in: S.A. Levin, T. G. Hallam, & L. J. Gross, eds., *Applied Mathematical Ecology*, Springer-Verlag, Berlin, pp 144–175.
10. Dobson, A. P. & P. J. Hilton, 1992. Regulation and stability of a free-living host–parasite system: *Trichostrongylus* in red grouse. II. Population models, *J. Animal Ecology* 61, 487–498.
11. Esteva, L., G. Rivas, and H. M. Yang. 2006. Modelling parasitism and predation of mosquitoes by water mites. *J. Math. Biol.*, 53, 540-555.
12. Fenton, A., T. Hakalahti, M. Bandilla, and E. T. Valtonen. 2006. The impact of variable hatching rates on parasite control: a model of an aquatic ectoparasite in a Finnish fish farm. *Journal of Applied Ecology*, 43, 660-668.
13. Hecker, K. R., M. R. Forbes, and N. J. Leonard. 2002. Parasitism of damselflies (*Enallagma boreale*) by gregarines: sex biases and relations to adult survivorship. *Canadian Journal of Zoology*, 80, 162-168.
14. Hoppensteadt, F. C. 1976. *Mathematical Methods of Population Biology*, Courant Inst. of Math. Sciences, New York University, NY.
15. Klingenberg, C. P., L. Barrington, H. Rosilind, B. A. Keddie, and J. R. Spence. 1997. Influence of gut parasites on growth performance in the water strider (Hemiptera: Gerridae). *Ecography*, 20, 29-36.
16. Levine, N. D. 1988. *The protozoan phylum Apicomplexa*, Vol. 1. CRC Press, Boca Raton, FL., 203p. Marcogliese, D. 2001. Implications of climate change for parasitism of animals in the aquatic environment. *Canadian Journal of Zoology*, 79, 1331-1352.

17. Logan, J. D. & W. R. Wolesensky, 2009. *Mathematical Methods in Biology*, John Wiley and Sons, New York.
18. Smith, J. M. 1974. *Models in Ecology*, Cambridge University Press, Cambridge UK.
19. Mangel, M. 2006. *The Theoretical Biologist's Toolbox*, Cambridge University Press, Cambridge UK.
20. McCallum, H. I. 1982. Infection dynamics of *Ichthyophthiris multifillis*, Parasitol. 85, 475–488.
21. McPeck, M. A. & B. L. Peckarsky, 1998. Life histories and strengths of species interactions: combining mortality, growth, and fecundity effects, Ecology 79(3), 867–879.
22. Milner, F. A & C. A. Patton, 1999. A new approach to mathematical modeling of host–parasite systems, Computers and Math. with Applics. 37, 93–110.
23. May, R. M. 1977. Togetherness among schistosomes: Its effects on the dynamics of infection, Math. Bios. 35, 301–343.
24. Nodtvedt, A., I. Dohoo, J. Sanchez, G. Conboy, L. DesCoteaux, G. Keefe, K. Leslie, and Campbell, J. 2002. The use of negative binomial modelling in a longitudinal study of gastrointestinal parasite burdens in Canadian dairy cows. Canadian Journal of Veterinary Research, 66, 249-257.
25. Nowak, M. A. 2006. *Evolutionary Dynamics*, Harvard University Press, Cambridge, MA.
26. Pal, P., and J. W. Lewis. 2004. Parasite aggregations in host populations using a reformulated negative binomial. Journal of Helminthology, 78, 57-61.
27. Percival, T. J., R. E. Clopton, & J. J. Janovy, 1995. Two new menosporine gregarines, *Hoplorhynchus acanthatholius* N. Sp. and *Steganorhynchus dunwoodyi* N. G., Sp, (Aplicomplexa: Eugregarinorida: Actinocephalidae) from coenagrionid damselflies (Odonata: Zygoptera), J. Euk. Microbiol. 42(4), 406–410.
28. Revie, C. W., E. Hollinger, G. Gettinby, F. Lees, and P. A. Heuch. 2007. Clustering of parasites within cages on Scottish and Norwegian salmon farms: alternative sampling strategies illustrated using simulation. Preventive Veterinary Medicine, 81, 135-147.
29. Richardson, S. & J. Janovy, 1990. *Actinocephalus carrilynnae* N. Sp. (Apicomplexa: Eugregarinorida) from the blue damselfly, *Enallagama civile* (Hagen), J. Protozool. 37, 567–570.

30. Roberts, L. S., and J. Janovy, Jr. 2009. *Foundations of Parasitology*, 8th Ed. McGraw-Hill, Dubuque, IA 701p.
31. Rodriguez, Y., and C. K. Omoto. 2007. Individual and population effects of eugregarine, *Gregarina niphandrodes*, on *Tenebrio molitor* (Coleoptera: Tenebrionidae). *Environmental Entomology*, 36, 689-693.
32. Westfall, M. J. Jr. & M. L. May. 1996. *Damselflies of North America*. Scientific Publishers, Washington, DC 649p.